

# Flow mechanism and heat transfer enhancement in longitudinal-flow tube bundle of shell-and-tube heat exchanger

LIU Wei<sup>†</sup>, LIU ZhiChun, WANG YingShuang & HUANG SuYi

School of Energy and Power Engineering, Huazhong University of Science and Technology, Wuhan 430074, China

**The flow disturbance and heat transfer mechanism in the tube bundle of rod baffle shell-and-tube heat exchanger were analyzed, on the basis of which and combined with the concept of heat transfer enhancement in the core flow, a new type of shell-and-tube heat exchanger with combination of rod and vane type spoiler was designed. Corresponding mathematical and physical models on the shell side about the new type heat exchanger were established, and fluid flow and heat transfer characteristics were numerically analyzed. The simulation results showed that heat transfer coefficient of the new type of heat exchanger approximated to that of rod baffle heat exchanger, but flow pressure drop was much less than the latter, indicating that comprehensive performance of the former is superior to that of the latter. Compared with rod baffle heat exchanger, heat transfer coefficient of the heat exchanger under investigation is higher under same pressure drop, especially under the high Reynolds numbers.**

shell-and-tube heat exchanger, tube bundle, rod baffle, vane-type spoiler, core flow, heat transfer enhancement

## 1 Introduction

Shell-and-tube heat exchangers are widely used in many fields, such as power plant, chemical engineering, oil refinery, etc., and some investigations have indicated that more than 70% of heat exchangers are of shell-and-tube type<sup>[1]</sup>. The baffles in heat exchangers have primary importance because they can not only support and fix the tube bundles, but also disturb the fluid. According to the flow direction in the shell side, shell-and-tube heat exchangers can be divided to three types, i.e., transverse flow type, longitudinal flow type and helical flow type. With different flow types, heat exchanger performances may present large difference. Heat transfer coefficient in the shell side has a heavy impact on overall heat transfer coefficient of heat exchanger. It is significant for studying the flow and heat transfer mechanism to reduce heat exchanger energy consumption, decrease heat transfer temperature difference, and improve heat exchanger performance.

Heat transfer enhancement (HTE) techniques can be classified as<sup>[2]</sup>: 1) reducing thermal boundary layer thickness; 2) increasing disturbance between fluid and surface; 3) extending heat transfer surface; and 4) treating heat transfer surface. Those techniques are all based on heat transfer surfaces or fluid near the surfaces, therefore, they are called boundary or surface enhancement techniques<sup>[3]</sup>.

Tube inserts are effective HTE techniques, and common tube inserts include twisted tape, wire coil, wire matrix, static mixture, and so on. In the traditional method, the tube is filled with inserts along the entire flow zone. As a result, heat transfer is enhanced with a cost of increasing flow resistance, especially in the turbulence zone<sup>[4–9]</sup>.

Received July 12, 2008; accepted May 5, 2009

doi: 10.1007/s11431-009-0237-7

<sup>†</sup>Corresponding author (email: w\_liu@hust.edu.cn)

Supported by the National Basic Research Program of China ("973" Project) (Grant No. 2007CB206903) and the National Natural Science Foundation of China (Grant No. 50721005)

Utilizing high effective heat transfer tube and disturbing fluid in the tube bundles are two major methods for heat transfer enhancement in the shell-and-tube heat exchangers. Corrugated tube, helical corrugated tube, tube with helical rib and converging-diverging tube are commonly used HTE tubes. Some of high performance HTE tubes can enhance heat transfer inside the tube, but it is not obvious in the shell side. The traditional shell-and-tube heat exchanger with segmental baffles have many disadvantages, such as high pressure drop, low heat transfer efficiency, harmful vibration caused by the shell-side flow normal to tube bundles. In order to improve the performance for shell-and-tube exchanger, heat exchangers with different types of baffles are developed, which have relatively higher heat transfer efficiency and relatively lower pressure drop, such as rod baffles and helical baffle exchangers<sup>[10-19]</sup>.

After taking some measures of heat transfer enhancement such as extended ribs, vortex generator and groove in the inner surface of confined space, the flow resistance will increase remarkably because the increase in fluid velocity gradient, viscous diffusion and momentum dissipation near the boundary makes the shear force, the friction between fluid and surface and the fluid dissipation work increase more or less. If the increase of flow resistance exceeds that of heat transfer, the overall performance for a heat transfer tube would decrease. To solve this problem in some cases of heat transfer enhancement, Liu et al.<sup>[20]</sup> proposed a principle of heat transfer enhancement in the core flow, and pointed out that if tube inserts can satisfy: 1) well-uniformed temperature in the core flow; 2) less fluid disturbance in the boundary layer; 3) small insert surface for disturbing fluid (or discontinuous insert surface for disturbing fluid), then a larger temperature gradient in the boundary layer can be made and high heat transfer efficiency and less increase in flow resistance can be resulted in. Liu et al.<sup>[21, 22]</sup> conducted a mechanism analysis and numerical investigation for tubes with partial filled with porous inserts in the core flow, and the results indicated that the comprehensive performance of enhanced tube for different fluid was better and the value of performance evaluation criteria (PEC) is much bigger than 1.

Numerical simulation for flow and heat transfer in the shell side of the rod baffle heat exchanger is conducted in this paper. On the basis of the principle for heat transfer enhancement in the core flow, a new type of

heat exchanger with rod-vane compound baffle is proposed and performance of flow and heat transfer is numerically investigated, and its performance comparison with rod baffle heat exchanger is also conducted.

## 2 Rod baffle heat exchanger

### 2.1 Mathematical and physical models

For the rod baffle heat exchanger with square-array tube bundles, a typical computational unit is sketched in Figure 1, by neglecting the effects of flow and heat transfer of the shell on the tube bundles, and supposing no heat and mass transfer between adjacent units.

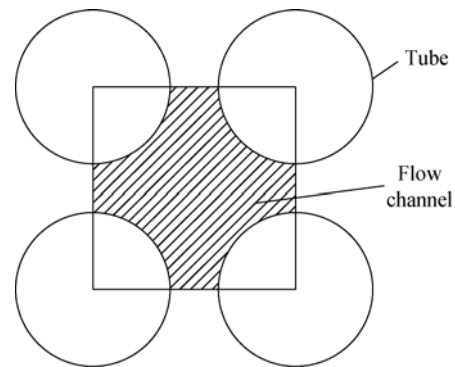


Figure 1 Flow unit duct of shell side of the rod baffle heat exchanger.

Some assumptions are made to establish the mathematical model: 1) physical properties of fluid are constant; 2) fluid is incompressible, isotropic and continuous; 3) fluid is Newton fluid; 4) the effect of gravity can be ignored. The RNG  $k-\varepsilon$  model combined with mass, momentum and energy conservation equations is employed to numerically simulate the flow and heat transfer process.

The common equations for flow and heat transfer are expressed as

$$\frac{\partial(\rho u_i \Phi)}{\partial x_i} = \frac{\partial}{\partial x_j} \left( \Gamma \frac{\partial \Phi}{\partial x_j} \right) + S. \quad (1)$$

The turbulence kinetic energy  $k$  and the dissipation rate  $\varepsilon$  for RNG  $k-\varepsilon$  turbulence model are expressed as the following transport equations

$$\frac{\partial(\rho k u_i)}{\partial x_i} = \frac{\partial}{\partial x_j} \left[ \alpha_k \mu_{\text{eff}} \frac{\partial k}{\partial x_j} \right] + G_k + \rho \varepsilon, \quad (2)$$

$$\frac{\partial(\rho \varepsilon u_i)}{\partial x_i} = \frac{\partial}{\partial x_j} \left[ \alpha_\varepsilon \mu_{\text{eff}} \frac{\partial \varepsilon}{\partial x_j} \right] + \frac{C_{1\varepsilon}^*}{k} G_k - C_{2\varepsilon} \rho \frac{\varepsilon^2}{k}. \quad (3)$$

In the above equations, for continuity equation,  $\Phi=1$ ,  $\Gamma=0$ ,  $S=0$ ; for momentum equation,  $\Phi=u, v, w$ ,  $\Gamma=\mu_{\text{eff}}=\mu+\mu_t$ ,  $S=-\frac{\partial p}{\partial x_i} + \frac{\partial}{\partial x_i} \left( \mu_{\text{eff}} \frac{\partial u_i}{\partial x_j} \right)$ ; for energy equation,  $\Phi=T$ ,  $\Gamma = \frac{\mu}{Pr} + \frac{\mu_t}{\sigma_T}$ ,  $S=0$ , where  $\mu_t = \rho C_\mu \mu \frac{k^2}{\varepsilon}$ ,  $C_\mu = 0.0845$ ,  $\alpha_k = \alpha_\varepsilon = 1.39$ ,  $C_{1\varepsilon}^* = C_{1\varepsilon} - \frac{\eta(1-\eta/\eta_0)}{1+\beta\eta^2}$ ,  $C_{1\varepsilon} = 1.42$ ,  $C_{2\varepsilon} = 1.68$ ,  $\eta = (2E_{ij} \cdot E_{ij})^{1/2} \frac{k}{\varepsilon}$ ,  $E_{ij} = \frac{1}{2} \left( \frac{\partial u_i}{\partial x_j} + \frac{\partial u_j}{\partial x_i} \right)$ ,  $\eta_0 = 4.377$ ,  $\beta = 0.012$ .  $\rho$  is fluid density,  $\mu$  is dynamic viscosity,  $Pr$  is fluid Prandt number,  $\sigma_T$  is turbulence prandt number,  $p$  is pressure,  $T$  is temperature,  $u, v$  and  $w$  are velocity components,  $\Gamma$  is generalized diffusion coefficient,  $\Phi$  is universal variable, and  $S$  is source item.

The computational zone was meshed with structured and unstructured grids. The zones near the rod or disturbance structure were meshed with unstructured grid, and the remaining zones were meshed with structured grid. By adopting this approach, we can not only improve the meshing quality but also reduce the meshing number. By studying the effects of different meshing approaches on the numerical results under same computational precision, we found that the meshing number of the blocking meshing method is much less than that of the one zone meshing method. Three grid densities (1607161, 1447491, 1217496) were adopted to obtain the grid independent solution. The results showed that the difference between the results of different grid systems was less than 3%. Considering both convergent time and solution precision, the grid system of 1217469 was adopted for the computational model.

SIMPLEC algorithm was used for pressure-velocity coupling, and QUICK scheme was chosen to discretize the momentum and energy equations. In this study, the fluid is water, and computational parameters are shown in Table 1.

**Table 1** Parameters for rod baffle heat exchanger

Tube type	Center space between tubes (mm)	Space between rod baffles (mm)	Rod diameter (mm)	Hydraulic diameter (mm)
$\phi 16 \times 2$	21	80, 120	5	19

After finding out velocity and temperature fields, heat transfer coefficient of the channel flow was calculated by  $h = q / (T_w - T_m)$ , where  $q$  is wall heat flux,  $T_w$  is wall averaged temperature, and  $T_m$  is fluid bulk temperature.

Friction coefficient was calculated by  $f = 2\Delta p \frac{D_e}{l} \frac{1}{\rho u_m^2}$ , where  $u_m$  is fluid average velocity,  $D_e$  is equivalent hydraulic diameter,  $l$  is tube length, and  $\Delta p$  is fluid pressure drop.

The performance evaluation criteria can be expressed as [2]

$$PEC = \frac{Nu / Nu_0}{(f / f_0)^{1/3}}, \quad (4)$$

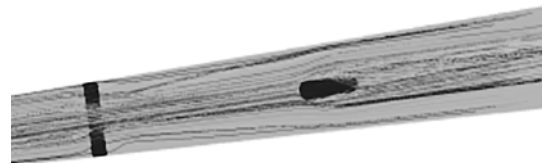
where  $Nu$  and  $Nu_0$  are Nusselt numbers for enhanced tube and smooth tube, respectively,  $f$  and  $f_0$  are friction coefficients for enhanced tube and smooth tube, respectively.

## 2.2 Results and analysis

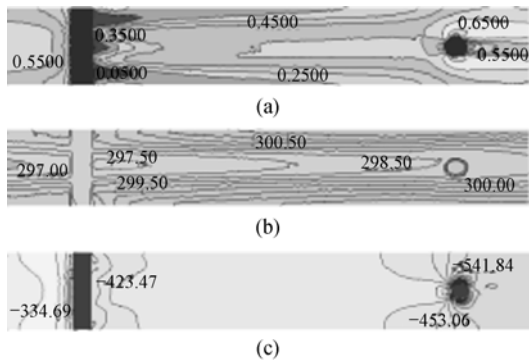
The HTE mechanism for the rod baffle heat exchanger can be stated as longitudinal disturbance effects of rod baffle on fluid in the shell side. As the rods touch the tubes only at each touch point, and the rod baffle is distributed longitudinally along the flow direction, they play a role of disturbing fluid and making fluid temperature uniform. As the fluid disturbance from the rod baffle is only localized, the increase in flow resistance is relatively small. This is very similar to heat transfer enhancement in the core flow [19]. So, by optimizing the support structure of the rod baffle, heat transfer can be enhanced with a relatively small increase in flow resistance.

Figure 2 shows the stream line of fluid flow in the computational unit, where it can be seen that the fluid can be disturbed longitudinally when it flows over the rod.

Figure 3 shows the velocity, temperature and pressure field distributions under  $Re=16000$ . From Figure 3, it can be observed that fluid temperature slowly increases and pressure slowly decreases from the inlet to the outlet, displaying a tendency of uniform. When fluid flows over



**Figure 2** Stream line for fluid flow over rod ( $Re=16000$ ).



**Figure 3** Pressure, temperature and velocity distributions in a certain flow section ( $Re=16000$ ). (a) Velocity distribution; (b) temperature distribution; (c) pressure distribution

the rods, due to fluid disturbance, velocity changes a lot and temperature becomes uniform, which means the effect of heat transfer enhancement is better.

Figures 4—7 show the changings of heat transfer coefficient,  $Nu$  number, friction coefficient and pressure drop under different  $Re$  numbers with rod spacings of 80 and 120 mm, respectively. It can be seen from the figures that with the increase in  $Re$  number, fluid disturbance is intensified and heat transfer is enhanced; as a result, both heat transfer and friction coefficients increase. Besides, with the increase of rod spacing, heat transfer and flow resistance decrease. The reason is that the fluid disturbance is reduced in the case of larger rod spacing.

As the deficiency of the rod baffle heat exchanger lies in that the fluid disturbance is not enough, its heat transfer performance will be limited. So, with the constant mass flow-rate in the shell side, in order to increase the fluid velocity in the shell side, one must reduce the shell diameter or the space between tubes, which may restrict the design and application for the rod baffle heat exchangers.

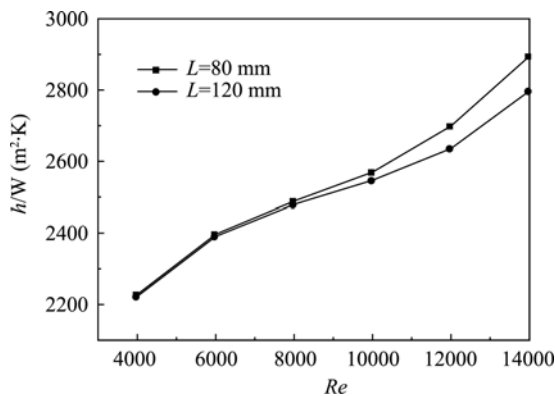


**Figure 4** Relations between  $Re$  number and heat transfer coefficient.

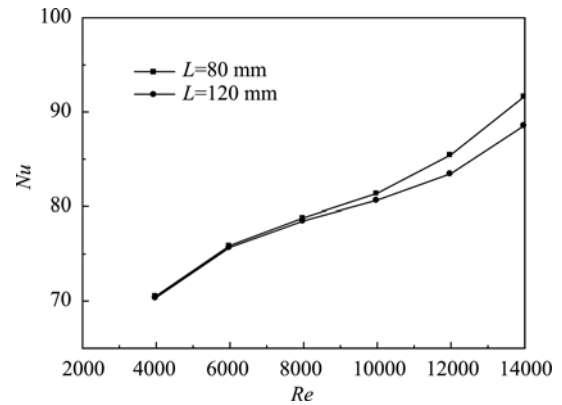


**Figure 5** Relations between  $Re$  number and  $Nu$  number.

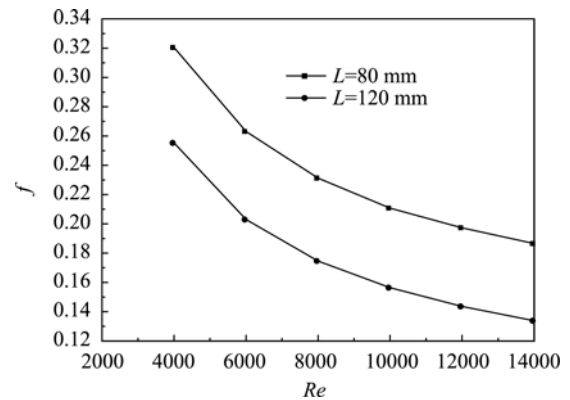


**Figure 6** Relations between  $Re$  number and friction coefficient.

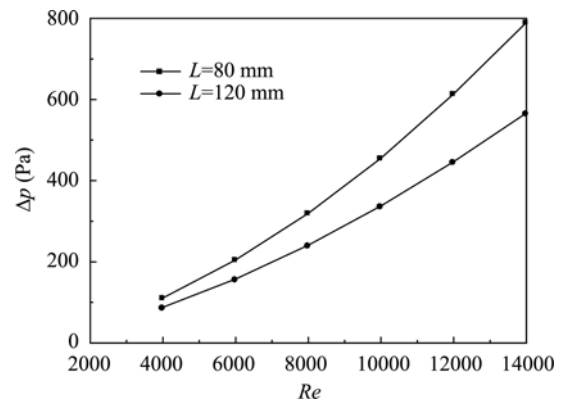


**Figure 7** Relations between  $Re$  number and pressure drop.

### 3 Rod-vane compound baffle heat exchanger

#### 3.1 Mathematical and physical models

According to the requirements of temperature uniform and fluid disturbance distribution for the HTE principle in the core flow, a more effective disturbance style to decrease flow resistance can be designed in the shell side of heat exchanger. With regards to this, vane type of

spoiler with proper intervals can be mounted along the flow direction. All vanes can be connected with a rod of 2 mm diameter, and the maximum vane width is 4 mm, vane height is 6 mm, and vane thickness is 1 mm. The transverse-section thickness of the vane is constant and twisted angle is 45° for reducing power dissipation. Figure 8 schematically shows a flow unit with rods and vanes in the shell side of the heat exchanger.

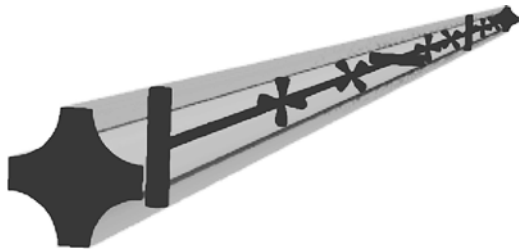


**Figure 8** Flow unit of shell side of the rod-vane compound baffle heat exchanger.

### 3.2 Results and analysis

Based on the physical model shown in Figure 8, flow and heat transfer in the rod-vane compound baffle heat exchanger was numerically investigated, and the comparison of numerical results between units of the rod baffle and the rod-vane compound baffle heat exchangers can be observed in Figures 9–13.

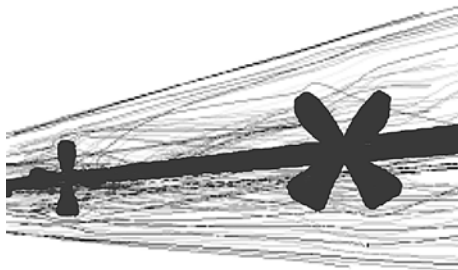


**Figure 9** Steam lines for the rod-vane compound baffle heat exchanger.

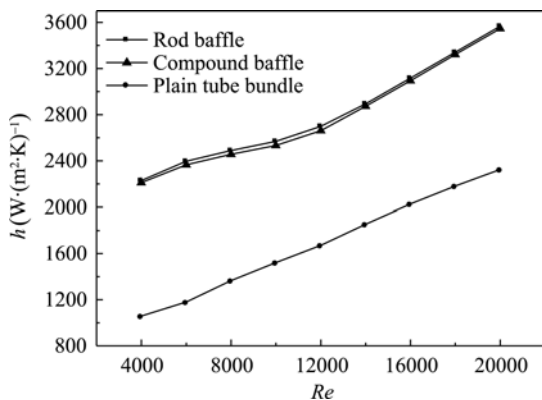


**Figure 10** Relations between  $Re$  number and heat transfer coefficient.

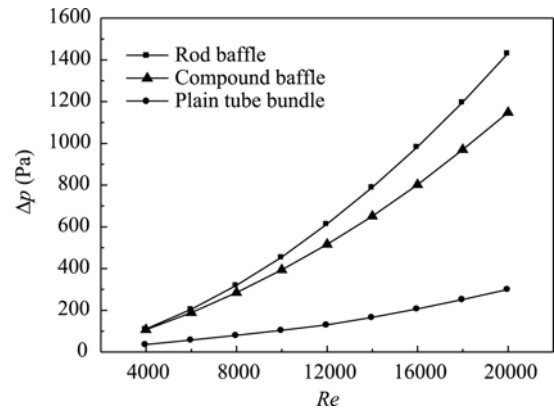


**Figure 11** Relations between  $Re$  number and pressure drop.

The flow behavior in the shell side of the new type heat exchanger is different than that of the traditional rod baffle heat exchanger. Figure 9 shows the stream lines over the rod-vane compound baffle. The flow pattern inside the flow unit with rod-vane compound baffle has been revealed as the swirl. As seen in Figure 9, the swirling flow takes place mainly in the center zone. Compared with the rod baffle heat exchanger, as fluid disturbance is more violent, temperature in the core flow is more uniform, which leads to a better effect of heat transfer enhancement. Furthermore, as disturbance surface of the vane type spoiler is relatively small and distributed, flow resistance can be reduced.

Figures 10 and 11 show the comparison of heat transfer coefficient and pressure drop under different  $Re$  numbers for the heat exchangers with rod-vane compound baffle, rod baffle and smooth tube bundles. As seen in the figures, the changing tendencies of heat transfer coefficients of the three types of heat exchangers are similar, and heat transfer coefficient of compound baffle of heat exchanger is slightly smaller than that of rod baffle heat exchanger, but both are better than that of smooth tube bundles. From Figure 11, it can be found that pressure drop of the heat exchanger with rod-vane compound baffle or rod baffle is larger than that of smooth tube bundles, but pressure drop of the heat exchanger with rod-vane compound baffle is smaller than that of heat exchanger with rod baffle. Furthermore, with the increase in  $Re$  number, the discrepancies between the two types of heat exchangers become larger.

Figures 12 and 13 show the comparison of  $Nu$  number and friction coefficient under different  $Re$  numbers for the heat exchangers with rod-vane compound baffle, rod baffle and smooth tube bundles. It can be found that

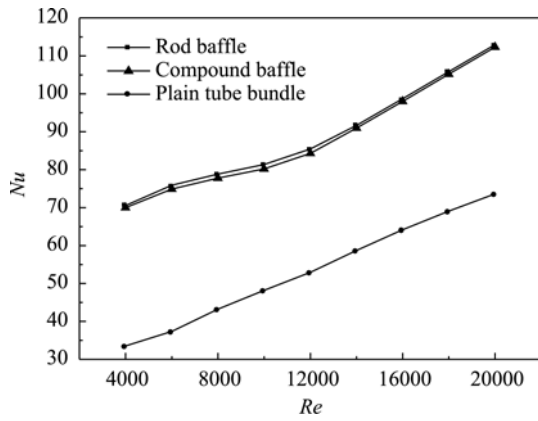


Figure 12 Relations between  $Re$  number and  $Nu$  number.

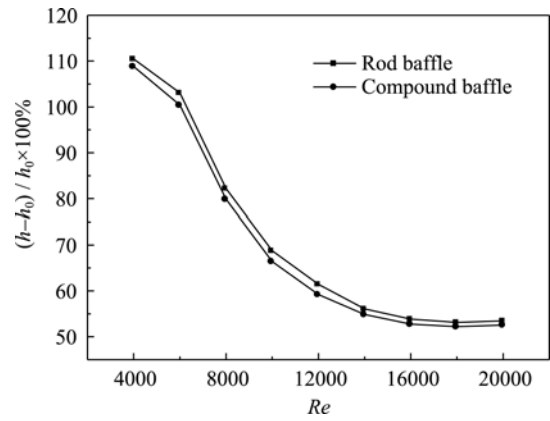


Figure 14 Relations between  $Re$  number and the changer rate of heat transfer coefficient.

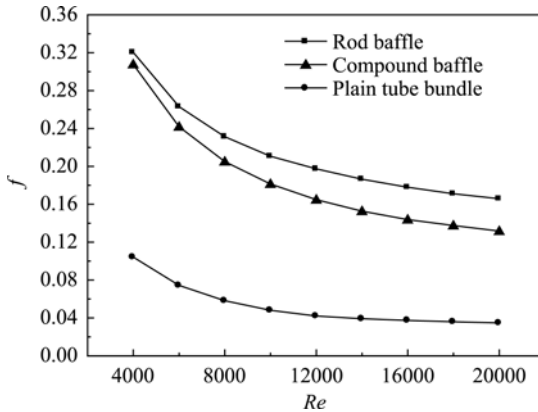


Figure 13 Relations between  $Re$  number and resistance coefficient.

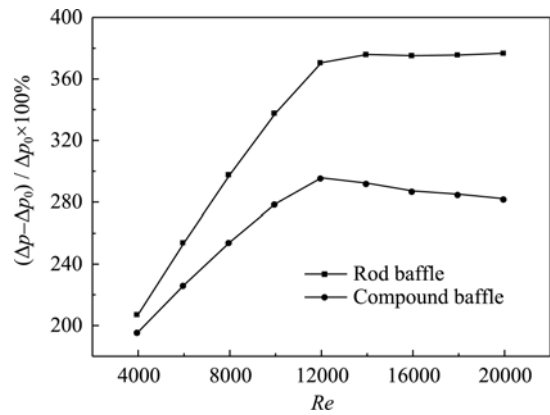


Figure 15 Relations between  $Re$  number and the changer rate of pressure drop.

with the increase in  $Re$  number, the  $Nu$  number also increases. From Figure 13, it can be seen that with the increase in  $Re$  number, friction coefficient decreases.

Figures 14 and 15 show the rate changes of heat transfer coefficients and pressure drops for heat exchangers with rod baffle and rod-vane compound baffles relative to that of heat exchanger with smooth tube bundles under different  $Re$  numbers. As seen in the figures, with the increase in  $Re$  number, heat transfer coefficient in the shell side decreases. As to flow resistance, with the increase in  $Re$  number, increase of amplitude of pressure drop is bigger at first, and then shows a tendency of decrease.

Figure 16 shows the change amplitudes of heat transfer coefficient and pressure drop of rod-vane compound baffle heat exchanger relative to that of rod baffle heat exchanger. As seen in the figure, in the scope of  $Re=4000-20000$ , increase of amplitude of heat transfer coefficient of rod baffle heat exchanger relative to heat exchanger with smooth tube bundles is 54%—110%,

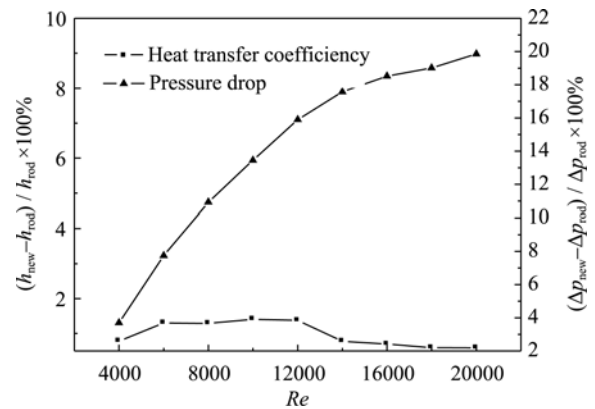


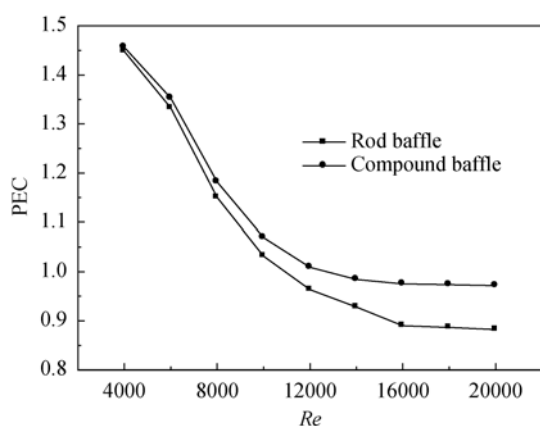
Figure 16 Change rates of the heat transfer coefficient  $h$  and pressure drop  $\Delta p$  of compound baffle heat exchanger relative to rod baffle exchanger under different  $Re$  numbers.

and increase amplitude of pressure drop is 207%—376%. For heat exchanger with rod-vane compound baffle, increases of amplitudes of heat transfer coefficient and pressure drop are 53%—109% and 195%—282%, re-

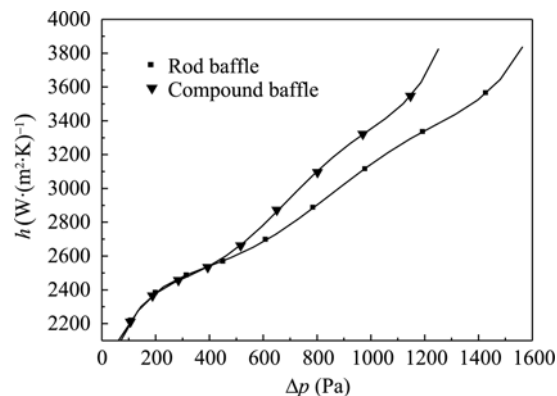
spectively. Compared with rod baffle heat exchanger, decreases of amplitudes of heat transfer coefficient and pressure drop for rod-vane compound baffle heat exchanger are 0.6%—1.4% and 4%—20%, respectively. Thus heat transfer coefficient of rod-vane compound baffles heat exchanger is close to that of rod baffle heat exchanger, but flow resistance of the former is smaller than that of the latter, and the difference in flow resistances between the two heat exchangers shows a tendency of increase in high  $Re$  number.

Figure 17 shows the changes of PEC values of heat exchangers with rod baffle and rod-vane compound baffle under different  $Re$  numbers. It can be found from the figure that in the scope of  $Re=4000$ — $20000$ , PEC values of rod baffle and rod-vane compound baffle heat exchangers are in the range of 0.8—1.5, but PEC value of the latter is always higher than that of the former. The difference in PEC values between the two types of heat exchangers shows a tendency of increase in high  $Re$  number. The reason for this is that with the increase in  $Re$  number, fluid disturbance caused by the rods is gradually intensified, and as a result, the flow resistance increases. For the rod-vane compound unit, however, fluid disturbance from the vane type spoiler mainly lies in the core flow, which leads to a relatively weak disturbance in the boundary layer. So, increase of amplitude of flow resistance is not so remarkable.

Figure 18 shows the changes of heat transfer coefficient vs. pressure drop for the heat exchangers with rod baffle and rod-vane compound baffle. As seen in the figure, under the same pressure drop or power dissipa-



**Figure 17** Relations between PEC of rod baffles and compound baffle heat exchangers and  $Re$  number.



**Figure 18** Relations between heat transfer coefficient and pressure drop.

tion, heat transfer coefficient of compound baffle is larger than that of rod baffle, and with the increase in fluid velocity, the discrepancy is more remarkable.

## 4 Conclusions

In summary, we have the following conclusions.

1) Under the guidance of the principle of heat transfer enhancement in the core flow, and with the analysis of the disturbance mechanism of longitudinal flow, a new type of high efficiency and low resistance heat exchanger with rod-vane compound baffle was designed and investigated numerically. The results show that for the same heat transfer coefficient, flow resistance in the shell side of rod-vane compound baffle heat exchanger is smaller than that of rod baffle heat exchanger. And for the same flow resistance, heat transfer performance of the former is better than that of the latter.

2) Compared with heat exchanger with smooth tube bundles in the  $Re$  number scope of 4000—20000, increases of amplitudes of heat transfer coefficient and pressure drop for heat exchanger with rod-vane compound baffle are 53%—109% and 195%—282%, respectively. But increases of amplitudes of heat transfer coefficient and pressure drop for heat exchanger with rod baffle are 54%—110% and 207%—376%, respectively.

3) By installing the vane type spoiler, the number of rod baffles and baffle rings can be reduced. By this way, not only can heat transfer be enhanced and flow resistance be decreased, but also the weight of heat exchanger can be decreased. As a result, the cost of heat exchanger can be reduced.

- 1 Qian S W. Handbook for Heat Exchanger Design (in Chinese). Beijing: Chemical Industry Press, 2002
- 2 Webb R L. Principles of Enhanced Heat Transfer. New York: Wiley, 1994
- 3 Bergles A E. ExHFT for fourth generation heat transfer technology. *Exp Thermal Fluid Sci*, 2002, 26(2-4): 335—344
- 4 Promvongse P, Eiamsa-ard S. Heat transfer behaviors in a tube with combined conical-ring and twisted-tape insert. *Int Comm Heat Mass Transfer*, 2007, 34(7): 849—859
- 5 Chang S W, Jan Y J, Liou J S. Turbulent heat transfer and pressure drop in tube fitted with serrated twisted tape. *Int J Thermal Sci*, 2007, 46(5): 506—518
- 6 Wang L K, Sunden B. Performance comparison of some tube inserts. *Int Comm Heat Mass Transfer*, 2002, 29(1): 45—56
- 7 Chang S W, Yang T L, Liou J S. Heat transfer and pressure drop in tube with broken twisted tape insert. *Exp Thermal Fluid Sci*, 2007, 32(2): 489—501
- 8 Naphon P. Heat transfer and pressure drop in the horizontal double pipes with and without twisted tape insert. *Int Comm Heat Mass Transfer*, 2006, 33(2): 166—175
- 9 Jin J, Liu P Q, Lin G P. Numerical simulation of heat transfer of latent functionally thermal fluid in tubes with coaxially inserted cylindrical bars in laminar. *Sci China Ser E-Tech Sci*, 2008, 51(8): 1232—1241
- 10 Mukherjee R. Use double-segmental baffles in the shell-and-tube heat exchangers. *Chem Eng Progress*, 1992, 88(11): 47—52
- 11 Li H, Kottke V. Analysis of local shell side heat and mass transfer in the shell-and-tube heat exchanger with disc-and-doughnut. *Int J Heat Mass Transfer*, 1999, 42(18): 3509—3521
- 12 Li H, Kottke V. Effect of baffle spacing on pressure drop and local heat transfer in shell-and-tube heat exchangers for staggered tube arrangement. *Int J Heat Mass Transfer*, 1998, 41(10): 1303—1311
- 13 Lei Y G, He Y L, Rui L, et al. Effects of baffle inclination angle on flow and heat transfer of a heat exchanger with helical baffles. *Chem Eng Process*, 2008, 47(12): 2336—2345
- 14 Lei Y G, He Y L, Pan C, et al. Design and optimization of heat exchangers with helical baffles. *Chem Eng Sci*, 2008, 63(17): 4386—4395
- 15 Dong Q W, Wang Y Q, Liu M S. Numerical and experimental investigation of shell side characteristics for rod baffle heat exchanger. *Appl Therm Eng*, 2008, 28(7): 651—660
- 16 Peng B, Qiang Q W, Zhang C, et al. An experimental study of shell-and-tube heat exchangers with continuous helical baffles. *J Heat Transfer*, 2007, 129(10): 1425—1431
- 17 Kara Y A, Guraras O. A computer program for designing of shell-and-tube heat exchangers. *Appl Therm Eng*, 2004, 24(13): 1797—1805
- 18 Costa André L H, Queiroz Eduardo M. Design optimization of shell-and-tube heat exchangers. *Appl Therm Eng*, 2008, 28(14-15): 1798—1805
- 19 Xie G N, Wang Q W, Zeng M, et al. Heat transfer analysis for shell-and-tube heat exchangers with experimental data by artificial neural networks approach. *Appl Therm Eng*, 2007, 27(5-6): 1096—1104
- 20 Liu W, Yang K, Nakayama A. Enhancing heat transfer in the core flow by forming an equivalent thermal boundary layer in the fully developed tube flow. In: *Sixth International Conference on Enhanced, Compact and Ultra-Compact Heat Exchangers: Science, Engineering and Technology*. Potsdam, Germany, 2007
- 21 Liu W, Yang K. Mechanism and numerical analysis of heat transfer enhancement in the core flow along a tube. *Sci China Ser E-Tech Sci*, 2008, 51(8): 1195—1202
- 22 Liu W, Ming T Z. Analysis for heat transfer enhancement in the core flow of a tube filled with porous media at different layers (in Chinese). *Proc CSEE*, 2008, 28(32): 66—71